Journal of Mathematical Modeling
Vol. 2, No. 1, 2014, pp. 1-21

JMM

Equidistribution grids for two-parameter convection–diffusion boundary-value problems

Jugal Mohapatra[†*]

[†]*Department of Mathematics, National Institute of Technology Rourkela- 769008, India*

Emails: jugal@nitrkl.ac.in, jugal.math@gmail.com

Abstract. In this article, we propose an adaptive grid based on mesh equidistribution principle for two-parameter convection-diffusion boundary-value problems with continuous and discontinuous data. A numerical algorithm based on an upwind finite difference operator and an appropriate adaptive grid is constructed. Truncation errors are derived for both continuous and discontinuous problems. Parameter uniform error bounds for the discrete solution are established. Numerical examples are carried out to show the performance of the proposed method on the adaptive grids.

AMS Subject Classification : 65L10, 65L12.
Keywords : Two-parameter singular perturbation problems, discontinuous coefficient, boundary and interior layers, finite difference methods, adaptive grids.

1 Introduction

Boundary value problems in mathematical physics which often depend upon small positive parameters $0 < \varepsilon, \mu \ll 1$ multiplied with highest order derivatives are called singularly perturbed differential equations. Such equations arise in semiconductor modelling, financial modelling, ion transport across biological membranes, population dynamics and many other applications

*Corresponding author.
Received : 23 February 2014, Revised: 12 April 2014, Accepted: 13 April 2014.

(see [3], [16], [18]) and the references therein. Typically, the solutions of these equations exhibit steep gradient in narrow regions either inside or near the boundaries of the domain; and these regions are known as interior or boundary layers. To solve these kinds of problems numerically in an efficient way, one has to use locally refined meshes that are fine in the layer regions and coarse outside the layers. Hence, singularly perturbed problems (in short, SPPs) present an important challenge for adaptive mesh techniques.

The numerical solution of two-parameter singularly perturbed boundary-value problems with smooth data have been studied by many authors including ([1], [8], [10], [11], [17]). Farrell et al. ([6], [7]) proposed numerical schemes for singularly perturbed one parameter problems with non smooth convective and source term. In [19], a robust numerical scheme is derived for two parameter problem with non smooth source term. In all these articles, the numerical schemes are applied on the piecewise-uniform Shishkin mesh. Though the Shishkin meshes are well-known for its simplicity and produce error estimates easily, one should know the location and width of the boundary or interior layers. In general, these information are not available for several problems, especially for nonlinear ordinary differential equations, and higher-dimensional partial differential equations.

To resolve the numerical difficulties arising from the boundary or interior layers, one should use more number of mesh points within the layers. If one can be able to do this automatically from the numerical solution calculated, then it is well and fine. Adaptive grids follow certain types of idea. A commonly used technique for determining the grid points is that they equidistribute a positive monitor function of the numerical solution over the domain and an obvious choice for adaptivity criterion is therefore the solution gradient (see [2], [12], [13]).

Recently, we derived a numerical scheme based on mesh equidistribution technique for two-parameter SPPs with continuous data in [14]. Also, we have obtained parameter-uniform error estimates. Here, in this article, we apply the adaptive grids obtained *viz.* the mesh equidistribution principle to two-parameter SPPs with continuous and discontinuous data. More precisely, we apply the classical upwind finite difference schemes to the SPPs on this adaptive grids. This approach has the advantage that it can be applied using little or no *a priori* information about the location and width of the boundary and interior layers. The proposed method is applied to some test problems to verify its applicability and efficiency. The numerical solution approximates the exact solution very well.

The structure of the paper is as follows. In Section 2, we state the

model problem for both continuous and discontinuous coefficients and also the comparison principle, stability result and some *a priori* estimates on the solution and its derivatives. Section 3 presents generation of the non-uniform grids through equidistribution principle, the upwind finite difference scheme and the corresponding bound of local truncation error for both continuous and discontinuous coefficients are given in Section 4. The numerical examples are presented in Section 5 to illustrate the applicability of the method.

We use the following notation

$$\partial\Omega = \{0, 1\}, \quad V^{(i)} = \frac{d^i V}{dx^i}, \quad \|u\| = \max_{\overline{\Omega}} |u(x)|.$$

Throughout this article C (sometimes subscripted) will denote the generic positive constant independent of nodal points, mesh size and the perturbation parameters ε, μ and N (the dimension of the discrete problem), which can take different values at different places, even in the same argument.

2 Properties of the exact solution

Here, we obtain the bounds on the continuous solution and its derivatives of the two-parameter SPPs with both continuous and discontinuous data.

2.1 SPPs with continuous data

Consider the following singularly perturbed two-parameter boundary-value problem:

$$\begin{cases} Lu(x) \equiv \varepsilon u''(x) + \mu p(x) u'(x) - q(x) u(x) = f(x), \quad x \in \Omega = (0, 1), \\ u(0) = A, \quad u(1) = B. \end{cases} \tag{1}$$

where $0 < \varepsilon, \mu \ll 1$ and p, q, f are sufficiently smooth functions such that $0 < \alpha \leq p(x)$ and $0 < \beta \leq q(x)$ on $\overline{\Omega} = [0, 1]$ and A, B are given constants. In general the BVP (1) possesses two boundary layer regions of different widths at $x = 0$ and $x = 1$. It is significant to observe that the two-parameter problem arises in the field of engineering, mathematical physics and applied mathematics. Such equation plays a crucial role in semiconductor modelling, financial modelling, population dynamics and in many other applications ([15], [16]).

For $\mu = 1$, the problem is one-dimensional convection diffusion problem and the solution exhibits a boundary layer of width $O(\varepsilon)$ at $x = 0$ and for

$\mu = 0$, we have one-dimensional reaction–diffusion problem and, in general the solution possesses boundary layers of width $O(\sqrt{\varepsilon})$ at $x = 0, 1$. Here the ratio of μ to $\sqrt{\varepsilon}$ is significant (see O'Malley [15]). Hence the analysis for the two parameter problem splits into two cases: $\mu \leq C_1\sqrt{\varepsilon}$ and $\mu \geq C_2\sqrt{\varepsilon}$. In the former case, the problem is close to single parameter reaction-diffusion case, while the latter case is more intricate.

The operator L of (1) satisfies the following comparison principle on $\overline{\Omega}$.

Lemma 1. *(Comparison Principle) Let $v \in \mathcal{C}^2(\overline{\Omega})$. If $v(0) \geq 0,\ v(1) \geq 0$ and $Lv(x) \leq 0\ \forall x \in\ \Omega,$ then $v(x) \geq 0,\ \forall x \in\ \overline{\Omega}$.*

An immediate consequence of this comparison principle is the following parameter uniform bound on the solution u of (1).

Lemma 2. *If u is the solution of the boundary value problem (1), then*

$$\|u\|_{\overline{\Omega}} \ \leq\ \max\{|u(0)|, |u(1)|\} + \frac{1}{\beta}\|f\|.$$

Proof. One can extend the proofs given in Doolan et al. [4] for two parameter problems. □

Lemma 3. *The derivatives $u^{(k)}$ of the solution u of (1) satisfy the following bounds*

$$\begin{aligned}
\|u^{(k)}\|_{\overline{\Omega}} \ &\leq\ \frac{C}{(\sqrt{\varepsilon})^k}\left(1 + \left(\frac{\mu}{\sqrt{\varepsilon}}\right)^k\right) \max\{\|u\|, \|f\|\}, \quad k = 1, 2\,. \\
\|u^{(3)}\|_{\overline{\Omega}} \ &\leq\ \frac{C}{(\sqrt{\varepsilon})^3}\left(1 + \left(\frac{\mu}{\sqrt{\varepsilon}}\right)^3\right) \max\{\|u\|, \|f\|, \|f'\|\},
\end{aligned}$$

where C depends only on $\|p\|,\ \|p'\|,\ \|q\|,\ \|q'\|$.

Proof. The detailed proof is given in [14] and [17]. □

In order to obtain parameter-uniform error estimate, we will decompose the solution into regular and singular components. We need to split the analysis into two cases depending on the ratio of μ to $\sqrt{\varepsilon}$. Starting with $\mu \leq C_1\sqrt{\varepsilon}$, we consider the solution decomposition as follows:

$$u = v + w_L + w_R. \tag{3}$$

where the function v is called the regular component. w_L and w_R are the left and right, layer components of the solution u satisfying the following set of equations:

$$\begin{cases} Lv = f, & v(0), v(1) \text{ suitably chosen }, \\ Lw_L = 0, & w_L(0) = u(0) - v(0), w_L(1) = 0, \\ Lw_R = 0, & w_R(0) = 0, w_R(1) = u(1) - v(1). \end{cases} \tag{4}$$

The boundary conditions of v are suitably chosen so that it satisfies the bounds:

$$\|v^{(i)}\| \leq C \quad i = 0, 1, 2 \quad \text{ and } \|v^{(3)}\| \leq \frac{C}{\varepsilon}. \tag{5}$$

The singular components w_L and w_R satisfy the bounds given in Lemma 3. However, one can also obtain the following sharper bounds on the exponential character of the two components.

Lemma 4. *The singular components w_L and w_R satisfy the bounds*

$$|w_L(x)| \leq Ce^{-\theta_1 x}, \tag{6}$$
$$|w_R(x)| \leq Ce^{-\theta_2(1-x)}, \tag{7}$$

where

$$\theta_1 = \frac{\mu\alpha + \sqrt{\mu^2\alpha^2 + 4\varepsilon\beta}}{2\varepsilon}, \qquad \theta_2 = \frac{-\mu P + \sqrt{\mu^2 P^2 + 4\varepsilon\beta}}{2\varepsilon},$$

($P = \|p(x)\|$ and θ_1, θ_2 are respectively the positive roots of the equations $\varepsilon\theta_1^2 - \mu\alpha\theta_1 - \beta = 0$ and $\varepsilon\theta_2^2 + \mu P\theta_1 - \beta = 0$)

Proof. Consider the barrier function $\psi^{\pm}(x) = Ce^{-\theta_1 x} \pm w_L(x)$. Choose C large enough so that the function are non-negative at $x = 0$. Now it is easy to calculate that $L\psi^{\pm}(x) \leq 0$ and applying the comparison principle Lemma 1, we obtain $|w_L(x)| < Ce^{-\theta_1 x}$. The proof for $w_R(x)$ is also similar. □

2.2 SPPs with discontinuous data

A singularly perturbed reaction-convection-diffusion equation in one dimension with a discontinuous coefficient of the first derivative term is considered on the unit interval $\Omega = (0, 1)$. A single discontinuity in the coefficient is assumed to occur at a point $d \in \Omega$. It is convenient to introduce the notation $\Omega^- = (0, d)$ and $\Omega^+ = (d, 1)$ and to denote the jump at d in any function

with $[w](d) = w(d+) - w(d-)$. The corresponding two point boundary value problem is as follows,

$$\begin{cases} \text{Find } u \in \mathcal{C}^0(\overline{\Omega}) \cap \mathcal{C}^1(\Omega) \cap \mathcal{C}^2(\Omega^- \cup \Omega^+) \text{ such that} \\ L_d u(x) \equiv \varepsilon u''(x) + \mu p(x) u'(x) - q(x) u(x) = f(x), \quad x \in \Omega = (0,1), \\ u(0) = A, \quad u(1) = B, \end{cases} \tag{8}$$

where $0 < \varepsilon \ll 1\,, 0 \le \mu \ll 1,\ q(x) \ge \beta > 0$ sufficiently smooth function in $\overline{\Omega}$ and p, f are sufficiently smooth function in $\Omega^- \cup \Omega^+$ where they satisfy

$$\begin{cases} \alpha_1^* > p(x) > \alpha_1 > 0, & x < d, \\ -\alpha_2^* < p(x) < -\alpha_2 < 0, & x > d, \\ |[p](d)| \le C, \quad |[f](d)| \le C. \end{cases} \tag{9}$$

The BVP (8)-(9) has a solution $u \in \mathcal{C}^0(\overline{\Omega}) \cap \mathcal{C}^1(\Omega) \cap \mathcal{C}^2(\Omega^- \cup \Omega^+)$ (see [6], [19]).

Let L_d denotes the differential operator given in (8) which satisfies the following comparison principle on $\overline{\Omega}$.

Lemma 5. *(Comparison Principle) Suppose a function* $w \in \mathcal{C}^0(\overline{\Omega}) \cap \mathcal{C}^2(\Omega^- \cup \Omega^+)$ *satisfies* $w(0) \ge 0$, $w(1) \ge 0$, $L_d w(x) \le 0$, $\forall x \in \Omega^- \cup \Omega^+$ *and* $[w]'(d) \le 0$, *then* $w(x) \ge 0\ , \forall\ x \in \overline{\Omega}\,.$

From Lemma 5, one can obtain the following stability results.

Lemma 6. *Let* u *be the solution of (8), then*

$$\|u\|_{\overline{\Omega}} \le \max\left\{ |u_0|, |u_1|, \frac{1}{\beta} \|f\|_{\overline{\Omega}\setminus\{d\}} \right\}.$$

Lemma 7. *Let* u *be the solution of (8) where* $|u(0)| \le C, |u(1)| \le C$, *then for all* $0 \le k \le 3$,

$$\|u^k\|_{\overline{\Omega}\setminus\{d\}} \le \frac{C}{\sqrt{\varepsilon}^k} \left\{ 1 + \left(\frac{\mu}{\sqrt{\varepsilon}}\right)^k \right\}.$$

Proof. Using the arguments as given in Farrell et al. [5] and in Shanthi et al. [19], one can prove the above Lemmas. □

We first consider the case $\mu \le C_1 \sqrt{\varepsilon}$. Define v_0, v_1, v_2 are the solutions of the following problems:

$$\begin{aligned} -q(x)v_0 &= f(x), \quad x \in \Omega^- \cup \Omega^+, \\ -q(x)v_1 &= \frac{-\mu}{\sqrt{\varepsilon}} p(x)v_0' - \sqrt{\varepsilon}v_0'', \quad x \in \Omega^- \cup \Omega^+, \\ -q(x)v_2 &= \frac{-\mu}{\sqrt{\varepsilon}} p(x)v_1' - \sqrt{\varepsilon}v_1'', \quad x \in \Omega^- \cup \Omega^+. \end{aligned} \tag{10}$$

Choose $v_3 \in \mathcal{C}^0(\overline{\Omega}) \cap \mathcal{C}^1(\Omega) \cap \mathcal{C}^2(\Omega^- \cup \Omega^+)$ such that

$$\begin{cases} Lv_3 = \dfrac{-\mu}{\sqrt{\varepsilon}} p(x)v_2' - \sqrt{\varepsilon}v_2'', \quad x \in \Omega^- \cup \Omega^+, \\ v_3(0) = v_3(1) = 0. \end{cases} \tag{11}$$

Let $v = v_0 + \sqrt{\varepsilon}v_1 + \varepsilon v_2 + \sqrt{\varepsilon}^3 v_3$. It is easy to verify that v satisfies

$$\begin{cases} Lv = f(x), \quad x \in \Omega^- \cup \Omega^+, \\ v(0) = v_0(0) + \sqrt{\varepsilon}v_1(0) + \varepsilon v_2(0), \\ v(d_-) = v_0(d_-) + \sqrt{\varepsilon}v_1(d_-) + \varepsilon v_2(d_-) + \sqrt{\varepsilon}^3 v_3(d_-), \\ v(d_+) = v_0(d_+) + \sqrt{\varepsilon}v_1(d_+) + \varepsilon v_2(d_+) + \sqrt{\varepsilon}^3 v_3(d_+), \\ v(1) = v_0(1) + \sqrt{\varepsilon}v_1(1) + \varepsilon v_2(1). \end{cases} \tag{12}$$

Similarly define the singular components w_L and w_R as the solution of the following equations respectively

$$\begin{cases} Lw_L = 0, \quad x \in \Omega^- \cup \Omega^+, w_L(0) = u(0) - v(0), w_L(1) = 0, \\ Lw_R = 0, \quad x \in \Omega^- \cup \Omega^+, w_R(0) = 0, w_R(1) = u(1) - v(1), \\ [w_L(d)] = -[v(d)] - [w_R(d)], \quad [w_L'(d)] = -[v'(d)] - [w_R'(d)]. \end{cases} \tag{13}$$

One can refer [8] for more details for the above decompositions.

Lemma 8. *The smooth component v satisfies the following bounds:*

$$\|v^k\|_{\overline{\Omega}\setminus\{d\}} \leq C\left(1 + \frac{1}{(\sqrt{\varepsilon})^{k-3}}\right), \quad 0 \leq k \leq 4.$$

Lemma 9. *The singular components w_L and w_R satisfy the following bounds:*

$$\|w_L^k\|_{\overline{\Omega}\setminus\{d\}} \leq \frac{C}{\sqrt{\varepsilon}^k}, \quad 1 \leq k \leq 3,$$

$$\|w_R^k\|_{\overline{\Omega}\setminus\{d\}} \leq \frac{C}{\sqrt{\varepsilon}^k}, \quad 1 \leq k \leq 3,$$

where

$$|w_L(x)| \leq \begin{cases} Ce^{-\theta_1 x}, & x \in \Omega^-, \\ Ce^{-\theta_1(x-d)}, & x \in \Omega^+, \end{cases}$$

$$|w_R(x)| \leq \begin{cases} Ce^{-\theta_2(d-x)}, & x \in \Omega^-, \\ Ce^{-\theta_2(1-x)}, & x \in \Omega^+, \end{cases} \qquad \theta_1 = \frac{C_1}{\sqrt{\varepsilon}}, \quad \theta_2 = \frac{C_2}{\sqrt{\varepsilon}}.$$

Proof. Using the arguments as given in Farrell et al. [5] and in Shanthi et al. [19], one can prove the above lemmas. □

It can be verified that $v + w_l + w_R$ satisfies the BVP (8). Consequently by the uniqueness, the solution of the BVP (8) can be written as

$$u(x) = \begin{cases} v^-(x) + w_L^-(x) + w_R^-(x), & x \in \Omega^-, \\ v^-(d_) + w_L^-(d_) + w_R^-(x) = v^+(d_+) + w_L^+(d_+) + w_R^+(d_+), \\ v^+(x) + w_L^+(x) + w_R^+(x), & x \in \Omega^+. \end{cases}$$

3 Grid equidistribution

The idea of adaptive grid generation is based on the equidistribution principle. A grid Ω_N is said to be equidistributing if

$$\int_{x_{j-1}}^{x_j} M\big(u(s), s\big)ds = \int_{x_j}^{x_{j+1}} M\big(u(s), s\big)ds, \quad j = 1, 2, \ldots, N-1. \tag{14}$$

where $M\big(u(x), x\big) > 0$ is called a monitor function. Equidistribution gives rise to a mapping $x = x(\xi)$ relating a computational coordinate $\xi \in [0, 1]$ to the physical coordinate $x \in [0, 1]$ defined by

$$\int_0^{x(\xi)} M\big(u(s), s\big)ds = \xi \int_0^1 M\big(u(s), s\big)ds. \tag{15}$$

The optimal choice of monitor function depends on the problem being solved, the numerical discretization being used. In practice, the monitor function is often based on a simple function of the derivatives of the unknown solution. Here we consider the monitor function as

$$M\big(u(x), x\big) = \left|\frac{du}{dx}\right|^{\frac{1}{m}}, \quad m \geq 2\ . \tag{16}$$

The effect of increasing m is to smooth the monitor function, which in turn leads to a smoother distribution of meshes.

3.1 SPPs with continuous data

3.1.1 Discrete problem

We will consider difference approximations of (1) on a non-uniform partition

$$\Omega_N = \{0 = x_0 < x_1 < x_2 < \cdots < x_{N-1} < x_N = 1\},$$

and denote $h_j = x_j - x_{j-1}$. Without loss of generality, we will assume that N is even. Given a mesh function Z_j, we define the following difference operators:

$$\begin{aligned} D^+Z_j &= \frac{Z_{j+1} - Z_j}{h_{j+1}}, \quad D^-Z_j = \frac{Z_j - Z_{j-1}}{h_j}, \\ D^+D^-Z_j &= \frac{2}{h_j + h_{j+1}}\left(\frac{Z_{j+1} - Z_j}{h_{j+1}} - \frac{Z_j - Z_{j-1}}{h_j}\right). \end{aligned}$$

The upwind finite difference discretization of (1) takes the following form:

$$\begin{cases} \left(L^N U_j\right) \equiv \varepsilon D^+D^-U_j + \mu p_j, D^+U_j - q_jU_j = f_j\,, \quad 1 \le j \le N-1, \\ U_0 = A, \quad U_N = B. \end{cases} \tag{17}$$

Here U_j denotes the approximation to $u(x_j)$, $p_j = p(x_j)$ and q_j, f_j are defined in a similar fashion.

Lemma 10. *(Discrete comparison principle). The system $L^NV_j = F_j$ with V_0 and V_N specified has a unique solution. If $L^NV_j < L^NZ_j$ for $1 \le j \le N-1$ with $V_0 < Z_0$ and $V_N < Z_N$, then $V_j < Z_j$ for $1 \le j \le N$.*

Proof. It is easy to verify that the matrix associated with L^N is an irreducible M-matrix and therefore, has a positive inverse. Hence, the result follows. □

We have the following discrete decomposition

$$U = V + W_L + W_R, \tag{18}$$

where the component are the solution of the following set of equations:

$$\begin{cases} L^NV = f(x_i), & V(0) = v(0), \quad V(1) = v(1), \\ L^NW_L = 0, & W_L(0) = w_L(0), W_L(1) = 0, \\ L^NW_R = 0, & W_R(0) = 0, W_R(1) = w_R(1). \end{cases} \tag{19}$$

3.1.2 Generation of grid

Considering the constant coefficient case for (1), using (16) in (15) we can get a relation between the non-uniform grid in physical space $\{x_j\}_{j=0}^{N}$, to the evenly distributed nodes $\xi_j = j/N$, $j = 0, 1, \ldots, N$ in the computational space. This yields the mapping

$$x_j = -\frac{m\varepsilon}{\alpha\mu} \ln\left(1 - \frac{\widehat{L}j}{N}\right), \quad j = 0, 1, \ldots, N, \tag{20}$$

where $\widehat{L} = 1 - \exp(1 - \alpha\mu/m\varepsilon)$. Now we state some conditions that are assumed through out the rest of the paper.

Assumptions

(*i*) Since we are interested in the limiting case that is as $\varepsilon \to 0$ and $\mu = O(\sqrt{\varepsilon})$, we assume there exists a constant k such that

$$\frac{m\varepsilon}{\alpha\mu} < k \ll 1, \tag{21}$$

where a is defined as before and hence there exist C_1 for which $1 > \widehat{L} > C_1 = 1 - \exp(-1/k)$.

(*ii*) We assume that

$$N\varepsilon \ll 1. \tag{22}$$

As we are interested in adaptive approach to the solution, the above assumptions are sensible.

Lemma 11. *We have the following bound:*

$$h_j < \frac{m\varepsilon}{\alpha\mu}, \qquad j = 1, 2, \ldots, N-1.$$

Proof. From (20) and using mean value theorem, we have for $j = 1, 2, \ldots, N-1$,

$$\begin{aligned} h_j \;=\; x_j - x_{j-1} \;&=\; -\frac{m\varepsilon}{\alpha\mu}\left[\ln(1 - \widehat{L}\xi_j) - \ln(1 - \widehat{L}\xi_{j-1})\right] \\ &=\; \frac{m\varepsilon L}{\alpha\mu N}\left[\frac{1}{1 - \widehat{L}\eta_j}\right], \quad \text{where} \quad \eta_j \in (\xi_{j-1}, \xi_j). \end{aligned}$$

Similarly ,

$$h_{j+1} = \frac{m\varepsilon\widehat{L}}{\alpha\mu N}\left[\frac{1}{1 - \widehat{L}\eta_{j+1}}\right], \quad \text{where} \quad \eta_{j+1} \in (\xi_j, \xi_{j+1}).$$

and since

$$\frac{1}{1-\widehat{L}\eta_j} < \frac{1}{1-\widehat{L}\eta_{j+1}}\ ,$$

it follows that $h_j < h_{j+1},\ j = 1, 2, \ldots, N-1$. Also, $\dfrac{1}{1-\widehat{L}\eta_j} < \dfrac{1}{1-\widehat{L}\xi_j}$.
Using the assumptions (21) and (22), we have

$$h_j < \frac{m\varepsilon\widehat{L}}{\alpha\mu N}\left[\frac{1}{1-\widehat{L}j/N}\right] = \frac{m\varepsilon}{\alpha\mu}\left[\frac{1}{N/\widehat{L}-j}\right] < \frac{m\varepsilon}{\alpha\mu}\left[\frac{1}{N-j}\right] .$$

Thus $h_j < m\varepsilon/\alpha\mu$ and we got the desired result. □

3.2 SPPs with discontinuous data

3.2.1 Discrete problem

Similarly the upwind finite difference discretization for the discontinuous case (8) takes the form

$$\begin{cases} \left(L_d^N U_j\right) \equiv \varepsilon D^+D^-U_j + p_j D^*U_j - q_j U_j = f_j\,, \quad 1 \le j \le N-1, \\ U_0 = A, \quad U_N = B, \\ D^-U_{N_k} = D^+U_{N_k}, \qquad \text{where} \quad x_{N_k} = d, \end{cases} \tag{23}$$

and

$$D^*Z_i = \begin{cases} D^+Z_i, & i < N_k, \\ D^-Z_i, & i > N_k. \end{cases}$$

Let us define V as

$$V(x_j) = \begin{cases} V^-(x_j), & 1 \le j \le N_k, \\ V^+(x_j), & N_k + 1 \le j \le N-1. \end{cases}$$

where the mesh functions V^- and V^+ which approximate v at left and right hand sides of the point of discontinuity $x = d$. Now V^- and V^+ are respectively the solutions of the following discrete problem:

$$\begin{cases} L_d^N V^-(x_j) = f(x_j) \quad \forall x_j \in \Omega_N^- \cup \Omega_N^+, \\ V^-(0) = v(0), \quad V^-(d) = v(d^-), \end{cases} \tag{26}$$

and

$$\begin{cases} L_d^N V^+(x_j) = f(x_j) \quad \forall x_j \in \Omega_N^- \cup \Omega_N^+, \\ V^+(d) = v(d^+), \quad V(1) = v(1). \end{cases} \tag{27}$$

Similarly, we can define W_L^-, W_L^+, W_R^- and W_R^+ which are respectively the solutions of the following problems:

$$\begin{aligned}
L_d^N W_L^-(x_j) &= 0 \quad \text{on} \quad 1 \le j \le N_k, \quad W_L^-(0) = w_L(0), \\
L_d^N W_L^+(x_j) &= 0 \quad \text{on} \quad N_k + 1 \le j \le N-1, \quad W_L^+(1) = w_L(1), \\
L_d^N W_R^-(x_j) &= 0 \quad \text{on} \quad 1 \le j \le N_k, \quad W_R^-(0) = w_R(0), \\
L_d^N W_R^+(x_j) &= 0 \quad \text{on} \quad N_k + 1 \le j \le N-1, \quad W_R^+(1) = w_R(1).
\end{aligned} \tag{28}$$

3.2.2 Generation of grid

To generate the grids, we can apply the same technique in the domain $\Omega^- \cup \Omega^+$ as used in the case of smooth coefficients. But due to the discontinuous convective term, there is a jump discontinuity at the point $x = d$ and also $\mu = O(\sqrt{\varepsilon})$, which results two boundary layers at both the end points of the domain. In view of these restrictions, we can form the grids with the help of the following relation.

$$x_j = -\frac{m\varepsilon}{\alpha\mu} \ln\left(1 - \frac{\widehat{L} j}{N}\right), \quad j = 0, 1, \ldots, N_k - 1, N_k + 1, \ldots, N, \tag{29}$$

where $\widehat{L}$ has been defined earlier. In order to make the point discontinuity $x = d$ as a grid point, we can take the weighted average of its neighboring points as $x_{N_k} = \dfrac{(H_k - \theta)x_{N_{k-1}} + \theta x_{N_{k+1}}}{H_k}$ where $0 < \theta < H_k = x_{N_{k+1}} - x_{N_{k-1}}$.

3.3 Adaptive algorithm

For practical point of view, the monitoring function has to be approximated from the numerical solution. Approximating (14) numerically results in the set of nonlinear algebraic equations

$$M_{j+\frac{1}{2}}(x_{j+1} - x_j) = M_{j-\frac{1}{2}}(x_j - x_{j-1}), \tag{30}$$

where $M_{j+\frac{1}{2}}$ is an approximation of $M(u(x_{j+\frac{1}{2}}), x_{j+\frac{1}{2}})$. For M given by (16), an obvious choice is

$$M_{j+\frac{1}{2}} = \left(\frac{U_{j+1} - U_j}{x_{j+1} - x_j}\right)^{\frac{1}{m}}, \quad j = 0, 1, \ldots, N-1.$$

The equations (17) and (23) with (30) should be solved simultaneously to obtain the solution U_j and the grids x_j.

4 Error analysis

Define the error as $e(x_j) = |U_j - u(x_j)|$. Here in this section, we wish to analyze the bounds on the error between the continuous and discrete solution.

4.1 SPPs with Continuous Data

4.1.1 Local truncation error

The local truncation error at the node x_j of (1) is given by

$$\tau_j = L^N U_j - (Lu)(x_j).$$

Using Peano-kernel theorem, the truncation error can be expressed as

$$\tau_j = \frac{\varepsilon}{h_j + h_{j+1}} \left[\frac{1}{h_{j+1}} \int_{x_j}^{x_{j+1}} (s - x_{j+1})^2 u'''(s) ds + \frac{1}{h_j} \int_{x_{j-1}}^{x_j} (s - x_{j-1})^2 u'''(s) ds \right] + \frac{\mu p_j}{h_{j+1}} \int_{x_j}^{x_{j+1}} (s - x_{j+1}) u''(s) ds. \quad (31)$$

Using the techniques used in [14] and [9], the local truncation error is given by

$$|\tau_j| < \frac{C}{\varepsilon N} \exp(-\alpha \mu x_j / m\varepsilon), \quad j = 1, 2, \ldots, N-1. \quad (32)$$

4.1.2 Bound on maximum point-wise error

Theorem 1. *Let $u(x)$ be the exact solution of (1) and let U_j be the discrete solution of (17) on the grid defined by (20). Then there exists a constant C, independent of N , ε and μ such that*

$$\max_{0 \le j \le N} |u(x_j) - U_j| \le C N^{-1}, \quad j = 0, 1, \ldots, N. \quad (33)$$

Proof. The detailed proof is given in [14]. □

4.2 SPPs with discontinuous data

4.2.1 Local truncation error

The truncation error at the interior mesh points $x_j \in \Omega_N$ can be given by

$$
\begin{aligned}
L_d^N e(x_j) &= L_d^N (U-u)(x_j) = f(x_j) - L_d^N u(x_j) \\
&= \Big[\varepsilon\big(\frac{d^2}{dx^2} - D^+D^-\big) + \mu p(x_j)\big(\frac{d}{dx} - D^*\big)\Big] u(x_j) \\
&= \Big[\varepsilon\big(\frac{d^2}{dx^2} - D^+D^-\big) + \mu p(x_j)\big(\frac{d}{dx} - D^*\big)\Big] \big(v(x_j) + w(x_j)\big).
\end{aligned}
$$

Lemma 12. *The regular component of the truncation error τ_{N_k} satisfies the following error estimate*

$$
|L_d^N (V-v)(x_j)| \leq CN^{-1}.
$$

Proof. It can be shown as

$$
\begin{aligned}
|L_d^N (V-v)(x_j)| &= |(L_d^N - L)v(x_j)| = C(x_{j+1} - x_{j-1})(\varepsilon\|v^3\| + \mu\|v^2\|) \\
&= C\varepsilon(x_{j+1} - x_{j-1}) \leq CN^{-1} \qquad (34)
\end{aligned}
$$

Using the bounds given in Lemma 8, one can obtain the above bounds. □

Again since $U(d) \leq C$, easy to check that $W_R(d) \leq C$ and $W_L(d) \leq C$. So, for $x_j \in \Omega^-$ we get $|W_L(x_j)| \leq |W_L(d)|N^{-1} \leq CN^{-1}$ and hence,

$$
\begin{aligned}
|W_L(x_j) - w_L(x_j)| &\leq |W_L(x_j)| + |w_L(x_j)| \\
&\leq |W_L(d)|N^{-1} + Ce^{-\theta_1 x} \\
&\leq CN^{-1}. \qquad (35)
\end{aligned}
$$

Similarly, one can also prove that

$$
|W_R(x_j) - w_R(x_j)| \leq CN^{-1}, \quad x_i \in \Omega^+. \qquad (36)
$$

All the above results as well as inequalities hold for both case $\mu \leq C\sqrt{\varepsilon}$ and $\mu \geq C\sqrt{\varepsilon}$. The following lemma establishes the truncation error at the jump discontinuity at $x = d$.

Lemma 13. *At the point of discontinuity d, the error $e(d)$ satisfies the following estimate*

$$
|(D^+ - D^-)e(d)| \leq \begin{cases} \dfrac{Cm}{\alpha\mu}, & \text{if} \quad \mu \leq C_1\sqrt{\varepsilon}, \\ \dfrac{Cm\mu}{\alpha\varepsilon}, & \text{if} \quad \mu \geq C_2\sqrt{\varepsilon}\ . \end{cases} \qquad (37)
$$

Proof. The above estimate can be obtained by using the bounds given in Lemma 11 and the techniques used in Shanthi et al. [19]. □

4.2.2 Bound on maximum point-wise error

Theorem 2. *Let $u(x)$ be the exact solution of (8) and let U_j be the discrete solution of (23) on the grid defined by (29). Then there exists a constant C, independent of N , ε and μ such that*

$$\max_{0\le j\le N} |u(x_j) - U_j| \le CN^{-1}, \quad j = 0, 1, \ldots, N. \tag{38}$$

Proof. First we will prove the result for the case $\mu \le C\sqrt{\varepsilon}$. From the equations (35),(36), Lemma 12 and applying the triangle inequality, it follows that

$$|L_d^N(U - u)(x_j)| \le CN^{-1}. \tag{39}$$

Consider the barrier function $\phi^{\pm}(x_j) = CN^{-1} + C\dfrac{h}{\varepsilon} \pm e(x_j)$ and using discrete comparison principle, we get

$$e(x_j) = |U(x_j) - u(x_j)| \le CN^{-1}, \quad \text{if } \mu \le C_1\sqrt{\varepsilon} \tag{40}$$

Similarly for the case $\mu \ge C_2\sqrt{\varepsilon}$, by suitably choosing a barrier function and using the above idea, one can obtain the desired result. □

5 Numerical results

To show the applicability and efficiency of the present method, it has been implemented to the following test problems.

Example 1. *Consider the singularly perturbed two parameter problem*

$$\begin{cases} \varepsilon u''(x) + \mu u'(x) - u(x) = -x, \quad x \in \Omega\,, \\ u(0) = 1, \quad u(1) = 0. \end{cases} \tag{41}$$

The exact solution is given by $u(x) = (x + \mu) + C_1 \exp(-m_1 x/2\varepsilon) - C_2 \exp((1 - x)m_2/2\varepsilon)$ where

$$m_{1,2} = \mu \pm \sqrt{\mu^2 + 4\varepsilon}, \quad C_1 = \frac{(1+\mu)\exp(m_2/2\varepsilon) + 1 - \mu}{1 - \exp(-\sqrt{\mu^2 + 4\varepsilon}/\varepsilon)}.$$
$$C_2 = \frac{1 + \mu + (1-\mu)\exp(-m_1/2\varepsilon)}{1 - \exp(-\sqrt{\mu^2 + 4\varepsilon}/\varepsilon)}.$$

Figure 1(a) displays the numerical and exact solution of Example 1 for $\varepsilon = 1e-3$, $\mu = 1e-7$ and $N = 256$; and Figure 1(b) represents the corresponding error. For any value of N, the maximum pointwise error

$E^N_{\varepsilon,\mu}$ is calculated by $E^N_{\varepsilon,\mu} = \|u(x_j) - U_j\|$, where u is the exact solution and U_j is the numerical solution. We use the double mesh principle to compute the rate of convergence as

$$\mathrm{p}^N = \log_2 \left(\frac{E^N_{\varepsilon,\mu}}{E^{2N}_{\varepsilon,\mu}} \right).$$

In Tables 1 and 2, we present the maximum pointwise error and the corresponding p^N for $\mu = 1e-2$ and $N = 32, 64, \ldots, 2048$. The results clearly show that this method is uniform convergence of order one. To have a proper visualization of the order of convergence, the loglog plots of the maximum pointwise error $E^N_{\varepsilon,\mu}$ are shown in Figure 2 for different values of ε and μ.

Example 2. *Consider the singularly perturbed two parameter problem with discontinuous coefficient*

$$\begin{cases} \varepsilon u''(x) + \mu p(x) u'(x) - u(x) = f(x), \quad x \in \Omega^- \cup \Omega^+, \\ u(0) = 0, \quad u(1) = 0, \end{cases} \tag{42}$$

where

$$p(x) = \begin{cases} x + 2, & 0 \le x \le 0.5, \\ -(2x+3), & 0.5 < x \le 1, \end{cases}$$

and

$$f(x) = \begin{cases} 2x + 1, & 0 \le x \le 0.5, \\ -(3x+4), & 0.5 < x \le 1. \end{cases}$$

The exact solution is not available for the BVP (2). In order to calculate the maximum point-wise error $G^N_{\varepsilon,\mu}$ and the rate of convergence q^N, we use interpolation. Define $\overline{U}^{10000}$ as the piecewise linear interpolation to U^N in Ω_N. Define,

$$G^N_{\varepsilon,\mu} = \max_{x_i \in \overline{\Omega}^N} |U^N - \overline{U}^{10000}| \quad \text{and} \quad q^N = \log_2 \left(\frac{G^N_{\varepsilon,\mu}}{G^{2N}_{\varepsilon,\mu}} \right).$$

Figure.3(a) displays the numerical solution and the interpolated solution of Example 2 for $\varepsilon = 1e-3$, $\mu = 1e-7$ and $N = 256$; and Figure 3(b) represents the corresponding error. Tables 3 and 4 represent the maximum pointwise error and the corresponding rate of convergence q^N. The loglog plots of the maximum pointwise error $G^N_{\varepsilon,\,\mu}$ are shown in Figure 4.

The tables and loglog plots highlight the error estimates obtained in Theorem 1 and Theorem 2. These results clearly show that the error estimate is optimal.

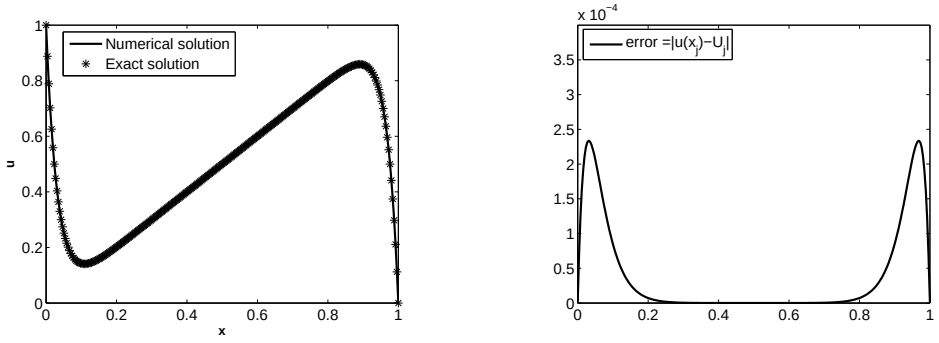

(a) Numerical solution and Exact solution. *(b) Error.*

Figure 1: *Numerical solution with exact solution and the error of the Example 1 for* $\varepsilon = 1e-3,\ \mu = 1e-7$ *and* $N = 256$.

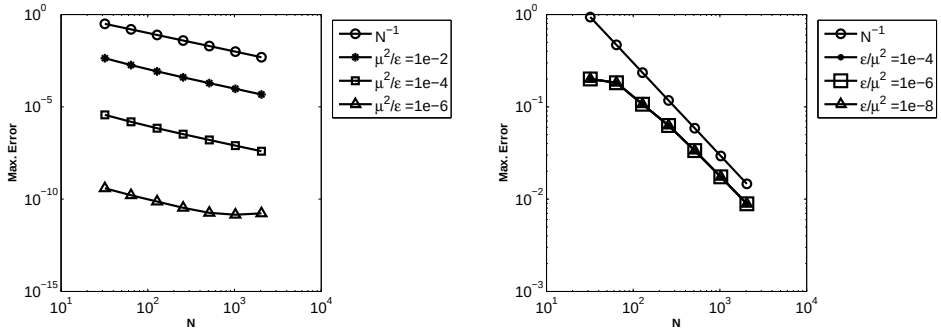

(a) μ^2/ε with $\mu = 1e-2$. (b) ε/μ^2 with $\mu = 1e-2$.

Figure 2: *Loglog plot of the maximum error for different values of* μ *and* ε *for Example 1.*

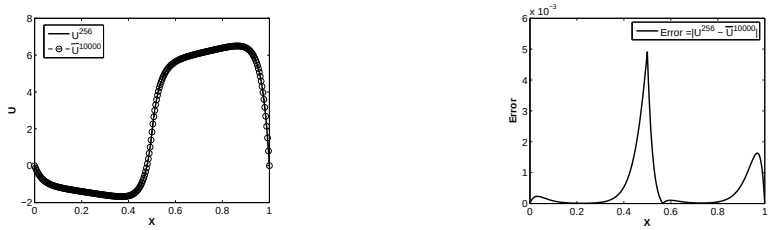

(a) Numerical solution and Interpolated solution. *(b) Error.*

Figure 3: *Numerical solution with interpolated solution and the error of the Example 2 for* $\varepsilon = 1e-3,\ \mu = 1e-7$ *and* $N = 256$.

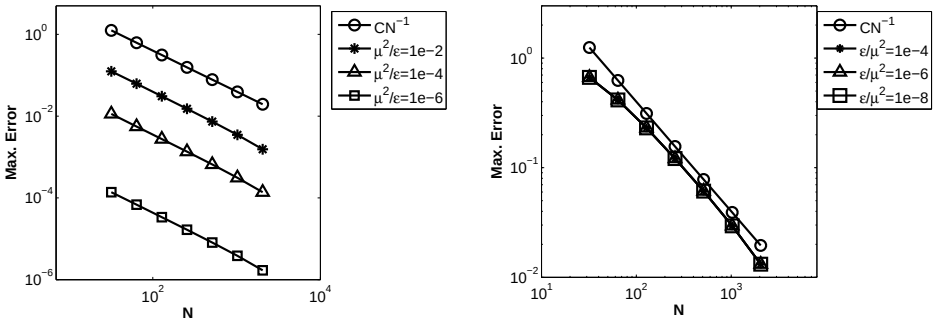

(a) μ^2/ε with $\mu = 1e-2$. (b) ε/μ^2 with $\mu = 1e-2$.

Figure 4: *Loglog plot of the maximum error for different values of* μ *and* ε *for the Example 2.*

Table 1: *Maximum point-wise errors* $E^N_{\varepsilon,\mu}$ *and the rate of convergence* p^N *generated for* $\mu = 1e-02$, $m = 2$ *for Example 1.*

ε/μ^2	Number of mesh points N						
	32	64	128	256	512	1024	2048
$1e-4$	2.0046e-1	1.8242e-1	1.0660e-1	6.6273e-2	3.3539e-2	1.7419e-2	8.8884e-3
	0.1361	0.7750	0.7663	0.9019	0.9452	0.9707	
$1e-6$	2.0047e-1	1.8244e-1	1.0662e-1	6.2687e-2	3.3548e-2	1.7424e-2	8.8909e-3
	0.1359	0.7496	0.7622	0.9019	0.9452	0.9706	
$1e-8$	2.0047e-1	1.8244e-1	1.0662e-1	6.2687e-2	3.3548e-2	1.7424e-2	8.8909e-3
	0.1359	0.7496	0.7622	0.9019	0.9452	0.9706	

Table 2: *Maximum point-wise errors* $E^N_{\varepsilon,\mu}$ *and the rate of convergence* p^N *generated for* $\mu = 1e-02$, $m = 2$ *for Example 1.*

μ^2/ε	Number of mesh points N						
	32	64	128	256	512	1024	2048
$1e-2$	4.3072e-3	1.8261e-3	8.2919e-4	3.9345e-4	1.9142e-4	9.4386e-5	4.6861e-5
	1.2380	1.1390	1.0755	1.0394	1.0201	1.0102	
$1e-4$	3.6557e-6	1.5357e-6	6.9522e-7	3.2928e-7	1.6007e-7	7.8881e-8	3.9159e-8
	1.2513	1.1433	1.0781	1.0406	1.0210	1.0103	
$1e-6$	3.8689e-10	1.6261e-10	7.3679e-11	3.4404e-11	1.7062e-11	8.5225e-12	4.2495e-12
	1.2505	1.1421	1.0987	1.0118	1.0014	1.0040	

Table 3: *Maximum point-wise errors* $G^N_{\varepsilon,\mu}$ *and the rate of convergence* q^N *generated for* $\mu = 1e-02$, $m = 2$ *for Example 2.*

ε/μ^2	Number of mesh points N						
	32	64	128	256	512	1024	2048
$1e-4$	6.6735e-1	4.1555e-1	2.3072e-1	1.2123e-1	6.1156e-2	2.9458e-2	1.3169e-2
	0.6834	0.8488	0.9284	0.9871	1.0539	1.1615	
$1e-6$	6.6737e-1	4.1556e-1	2.3073e-1	1.2123e-1	6.1159e-2	2.9459e-2	1.3170e-2
	0.6834	0.8488	0.9284	0.9871	1.0539	1.1615	
$1e-8$	6.6737e-1	4.1556e-1	2.3073e-1	1.2123e-1	6.1159e-2	2.9459e-2	1.3170e-2
	0.6834	0.8488	0.9284	0.9871	1.0539	1.1615	

Table 4: *Maximum point-wise errors* $G^N_{\varepsilon,\mu}$ *and the rate of convergence* q^N *generated for* $\mu = 1e-02$, $m = 2$ *for Example 2.*

μ^2/ε	Number of mesh points N						
	32	64	128	256	512	1024	2048
$1e-2$	1.2495e-1	6.2067e-2	3.0756e-2	1.5165e-2	7.3770e-3	3.4877e-3	1.5445e-3
	1.0095	1.0129	1.0201	1.0397	1.0807	1.1752	
$1e-4$	1.1321e-2	5.5732e-3	2.7514e-3	1.3536e-3	6.5799e-4	3.1100e-4	1.3770e-4
	1.0225	1.0183	1.0234	1.0407	1.0812	1.1753	
$1e-6$	1.3803e-4	6.8285e-5	3.3796e-5	1.6648e-5	8.0977e-6	3.8286e-6	1.6955e-6
	1.0153	1.0147	1.0215	1.0398	1.0807	1.1751	

6 Conclusion

This article presents an adaptive grid technique *viz.* mesh equidistribution for two-parameter SPPs with continuous and discontinuous data. The monitor function sends enough number of grids inside the boundary layers. Indeed, the solution of the two-parameter SPPs possesses boundary layers of different widths at both the end points of the domain. The present method is the most general step up to solve such types of problems. In the discontinuous data case, there is an interior layer in addition to the presence of boundary layers. This is also taken care by the adaptive mesh. The efficiency and applicability of the proposed method can be easily seen from the numerical results presented in the previous section.

Acknowledgments

The author expresses his sincere thanks to the anonymous referees for their valuable comments and suggestions. This research work is supported by the Department of Science & Technology, Government of India under research grant no. SERB/F/7053/2013-14.

References

[1] B.S. Attili, *Numerical treatment of singularly perturbed two point boundary value problems exhibiting boundary layers,* Commun. Nonlinear Sci. Numer. Simulat. **16** (2011) 3504–3511.

[2] M.G. Beckett and J.A. Mackenzie, *Converenges analysis of finite differences approximations on equidistribted grids to a singularly perturbed boundary value problem,* Appl. Numer. Math. **35** (166) (2000) 87–109.

[3] J. Chen and R.E. O'Malley JR, *On the asymtotic solution of a two parameter boundary value problem of chemical reactor theory,* SIAM. J. Appl. Math. **26** (4) (1974) 717–729.

[4] E.P. Doolan, J.J.H. Miller and W.H.A. Schildres, *Uniform Numerical Methods for Problems with Initial and Boundary Layers*, Boole Press, Dublin, 1980.

[5] P.A. Farrell, A.F. Hegarty, J.J.H. Miller, E. O'Riordan and G.I. Shishkin, *Robust Computational Techniques for Boundary Layers*, Chapman & Hall/CRC Press, 2000.

[6] P.A. Farrell, A.F. Hegarty, J.J.H. Miller, E. O'Riordan and G.I. Shishkin, *Global maximum norm parameter-uniform numerical method for a singulaly perturbed convection-diffusion problem with discontunuous convection coefficient,* Math. Comput. Modelling. **40** (2004) 1375–1392.

[7] P.A. Farrell, A.F. Hegarty, J.J.H. Miller, E. O'Riordan and G.I. Shishkin, *Singulaly perturbed convection-diffusion problem with boundary and weak interior layers,* J. Comput. Appl. Math. **166** (2004) 133–151.

[8] J.L. Gracia, E. O'Riordan and M.L. Pickett, *A parameter robust second order numerical method for singularly perturbed two parameter problem,* Appl. Numer. Math **56** (2006) 962–980.

[9] R.B. Kellogg and A. Tsan, *Analysis of some differences approximations for a singular perturbation problem without turning point,* Math. Comp. **32** (144) (1978) 1025–1039.

[10] T. Linβ, *Layer-adapted meshes for one-dimensional reaction-convection-diffusion problems,* J. Numer. Math. **12** (2004) 193–205.

[11] T. Linβ and H. G. Roos, *Analysis of finite difference scheme for a singularly perturbed problem with two small parameters,* J. Math. Anal. Appl. **289** (2) (2004) 355–366.

[12] J. Mackenzie, *Uniform converenges analysis of an upwind finite differences approximation of a convection-diffusion boundary value problem on an adaptive grid,* IMA J. Numer Anal. **19** (1999) 233–249.

[13] J. Mohapatra and S. Natesan, *Parameter–uniform numerical method for global solution and global normalized flux of singularly perturbed*

boundary value problems using grid equidistribution, Comput. Math. Appl. **60** (7) (2010) 1924–1939.

[14] J. Mohapatra and M. K. Mahalik, *Parameter-uniform convergence analysis of finite difference scheme for two-parameter singular perturbation problems on equidistributed grids,* Submitted for Publication.

[15] R.E. O'Malley, *Two parameter singular perturbation problems for second order equations,* J. Math. Mech. **16** (10) (1967) 1143–1164.

[16] R.E. O'Malley, *Introduction to Singular Perturbations*, Academic Press, New York, 1974.

[17] E. O'Riordan, M.L. Pickett and G.I. Shishkin. *Singularly perturbed problems modelling-reaction-convection-diffusion processes,* Comput. Meth. Appl. Math. **3** (3) (2003) 424–442.

[18] H.G. Roos, M. Stynes and L. Tobiska, *Numerical Methods for Singularly Perturbed Differential Equations*, Springer, Berlin, 1996.

[19] V. Shanthi, N. Ramanujam and S. Natesan. *Fitted mesh method for singularly perturbed reaction convection-diffusion problems with boundary and interior layers,* J. Appl. Math. Computing **22** (1-2) (2006) 49–65.